Haptic Mushroom: a 3-DoF shape-changing encounter-type haptic device with interchangeable end-effectors

Lisheng Kuang, Francesco Chinello, Paolo Robuffo Giordano, Maud Marchal, Claudio Pacchierotti

Haptic Mushroom: a 3-DoF shape-changing encounter-type haptic device with interchangeable end-effectors

Lisheng Kuang
CNRS, Univ Rennes, Inria, IRISA
Rennes, France
lisheng.kuang@irisa.fr

Francesco Chinello
Dept. Business Dev. and Technology
Aarhus University
Herning, Denmark
chinello@btech.au.dk

Paolo Robuffo Giordano
CNRS, Univ Rennes, Inria, IRISA
Rennes, France
prg@irisa.fr

Maud Marchal
Univ Rennes, INSA Rennes, Inria, IRISA
Rennes, France
maud.marchal@irisa.fr

Claudio Pacchierotti
CNRS, Univ Rennes, Inria, IRISA
Rennes, France
claudio.pacchierotti@irisa.fr

***Abstract*—This paper presents the Haptic Mushroom, a grounded encounter-type haptic device with interchangeable end-effectors. It is composed of a three-leg parallel self-constrained mechanism connecting a lower static platform to an upper moving platform. The upper platform moves over the surface of a sphere centered on the lower one. The legs are attached to the moving platform through three joints, which are in turn driven through a spiral cam, finally actuating the chosen end-effector. As a representative example, we consider a soft end-effector, able to change its curvature, and a rigid origami-inspired end-effector, able to change its shape from flat to sharp. However, the device is designed to support a wide range of end-effectors. The paper describes the device and presents the kinematic characterisation of the two end-effectors. We carry out a perceptual experiment, enrolling 12 participants, evaluating the capability of the soft end-effector to render curvatures. Finally, we present a use case where the device is used as an encounter-type haptic interface during interactions with virtual objects.**

***Index Terms*—grounded haptic interfaces, encounter-type haptics, shape-changing devices**

I. Introduction

Grounded haptic devices have been employed for a wide range of applications, from space to surgical robotics, from rehabilitation to industrial training. They include popular commercial haptic systems such as the Virtuose (Haption, FR), Omega.x (Force Dimension, CH), Falcon (Novint, USA) and the Phantom (3D Systems, USA) series, but also grounded self-reconfiguring tangibles, encounter-type interfaces, shape-changing devices, and table-top haptic systems [1]–[5]. Such haptic devices can be categorized in different ways, according to their, e.g., peak force, bandwidth, workspace, rendering capabilities, form factor [6]–[8].

However, there exists no "perfect" haptic interface, as each situation needs a different set of features. For example, an interface might perform well at rendering an object's curvature, but it may be a worse choice than others if such a feature is not important for the considered task. Similarly, the perceptual relevance of the rendered haptic sensations with respect to the application at hand also needs to be considered for deciding which types of haptic stimuli are more important to convey. Indeed, as providing different types of haptic cues usually means bulkier (and more expensive) interfaces, it is rare to find haptic devices able of convey a large set of haptic sensations [7], [8]. This limitation is particularly daunting in Virtual Reality (VR), where the limited actuation capabilities of the haptic device in use should not limit the design choices for the virtual content [9]. For this reason, modular and reconfigurable approaches, where it is easy to modify, upgrade, and adapt the haptic system to fit the scenario's needs are increasingly popular [1], [10], [11].

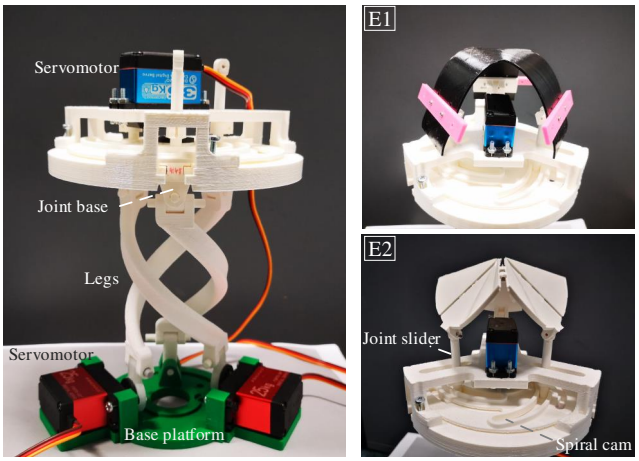

Fig. 1. The proposed 3-DoF shape-changing encounter-type haptic device. (Left) Structure of the device (no end-effector attached yet). The lower/base platform (green in the Figure) is fixed, while the moving platform moves over the surface of a sphere. As a representative example, we considered a (E1) soft end-effector, able to change its curvature, and (E2) a rigid origami-inspired end-effector, able to change its shape from flat to sharp.

This paper presents the Haptic Mushroom, a 3-degrees-of-freedom (3-DoF) encounter-type grounded kinesthetic device, shown in Figs. 1 and 2. It is composed of two platforms, one fixed on an external support and one moving, connected by a three-leg parallel self-constrained mechanism. The legs move the moving platform around the surface of a sphere centered on the lower fixed base. The legs are attached to the moving platform on joint bases, which are in turn driven by one additional servomotor through a spiral cam. Finally, the chosen end-effector is attached to three vertical joint sliders rigidly installed on the actuated sliding guides. The end-effector can be designed according to the task at end, providing the necessary feedback information. In this paper, as a representative example, we present a soft end-effector, able to render the sensations of interacting with different curvatures, and a rigid origami-like end-effector, able to render the sensations of interacting with different folding shapes.

With respect to other works in the literature, this device combines the characteristics of shape-changing displays and encounter-type systems. Moreover, its modular design enables the easy and quick replacement of the end-effector to best fit the rendering requirements of the environment at hand.

II. Related Work

This Section summarizes the state of the art around the proposed work, focusing on encounter-type grounded haptic interfaces and shape-changing/reconfigurable grounded systems.

Encounter-type grounded haptics. Encountered-type haptic systems convey haptic sensations by reactively positioning a (tangible) end-effector for the human user to encounter. This type of haptic display enables users to have unconstrained, free-hand contact with a tangible object provided by a robotic device, differently from more standard haptic devices in which users are required to always contact the end-effector. Mercado et al. [1] presented a comprehensive survey on this topic, proposing a taxonomy for classifying hardware types, as well as an analysis of haptic feedback most used in this context. For example, Mercado et al. [12] attached a cylindrical spinning tangible object to a robotic arm end-effector; the sensation of touching a virtual surface is achieved by coupling the movement of the robot with the sliding movement of the tangible object under the users' fingers. Similar recent approaches using a robotic arm to present a tangible prop to the user have been presented in [13]–[15]. Alternatively, Suzuki et al. [3] employed multiple tabletop-size ground mobile robots to recreate the sensation of interacting with a virtual environment. The mobile robots move on a table and can change their height and orientation to haptically render various surfaces and objects as the user contacts them. Similar recent approaches using ground mobile robots to present a tangible prop to the user have been presented in [16], [17].

Grounded shape-changing haptics. Actuated tangible user interfaces take advantage of our inherent spatial reasoning skills to haptically manipulate the environment around us. Among these interfaces, shape-changing devices are systems that allow for more general purpose shape change. Researchers have employed such systems for directly touching the (shape-changing) surface [18]–[20], manipulating tangible objects through said surface [21], and remotely interacting through gestures [22]. For example, Poupyrev et al. [19] proposed an electromechanical device consisting of a 2D array of movable light guides, whose height and color can be independently controlled to display images, shapes, and haptic sensations. Nakagaki et al. [20] presented a high-quality feedback 10×5 shape-changing display using linear actuators, able to both detect and apply dynamic force feedback at each pin. Follmer et al. [21] designed a shape display featuring dynamic affordances, constraints, and actuation of passive objects, using 30×30 actuated polystyrene pins in a 381×381 mm area. Blackshaw et al. [22] proposed an array of 120 actuated and instrumented pins, whose motion was controlled by the human user through a series of gestures captured by a depth camera installed above the array.

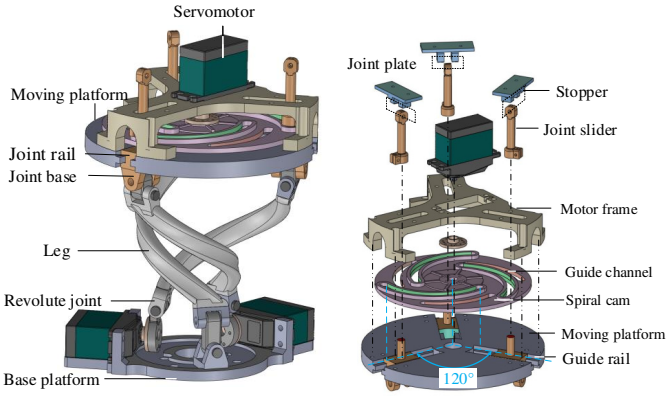

(a) CAD design (b) Upper moving platform

Fig. 2. Schematics of the proposed device. (a) CAD design. (b) Assembly view of the upper moving platform of the device, which includes the spiral cam mechanism that actuates the three joint sliders driving the end-effectors.

III. Device description and implementation

A. Device design and structure

The design of this device is inspired by the anti-parallelogram mechanism originally presented in [23] and later adopted in [24], [25]. A prototype of the device is shown in Fig. 1, its schematic design is depicted in Fig. 2, and a set of representative movements are shown in Fig. 3.

Three identical supporting legs are evenly placed around the the z axis of two platforms, forming an interlaced structure with no interference between them. The lower base platform is fixed on an external support and houses two servomotors, while the moving platform moves. The end of each leg is connected to the platforms through four serial revolute joints, indicated as R_i, $i = 1, 2, 3, 4$, in Fig. 3 (State b), forming three legs chained with four rotational joints (3-4R) coupling parallel mechanism. With this configuration, the three legs (actuated by two servomotors only) impose two degrees-of-freedom of

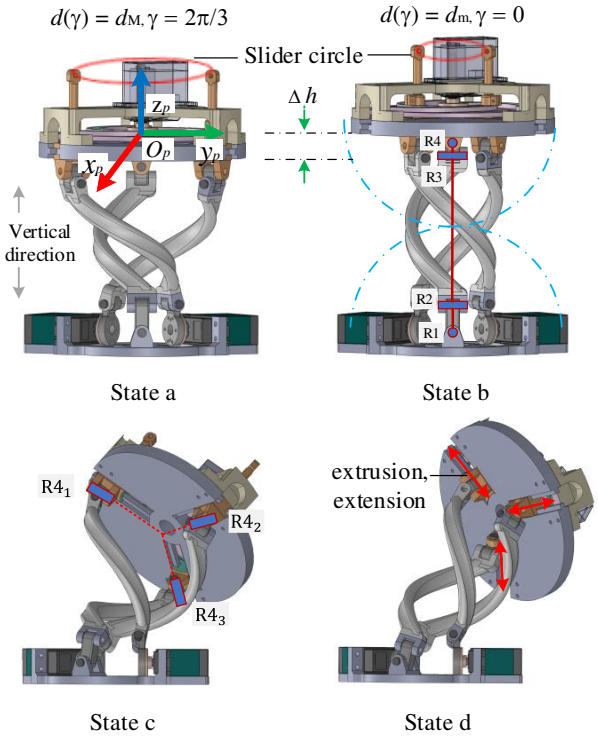

Fig. 3. Representative movements of the device. The three joint sliders are actuated within a circle (red) centered at the center of the moving platform. When the spiral cam rotates, the height of the platform and the radius of the abovementioned circle change. The blue dashed ellipses indicate the rolling motion of the platform. R_i represent the revolute joints of the three legs. (States a and b) The device is in a upright configuration and the spiral cam rotates to lower the moving platform and reduce the diameter of the slider circle. When equipped with the soft Y-shaped end-effector, this movement increases the curvature of the end-effector surface, as also shown in Fig. 4. (States c and d) The same movement as before but with the device in a bent configuration.

motion to the mechanism, as also analysed in [26]. When the base platform is fixed on an external support (as in Fig. 2), the motion of the moving platform is confined on the surface of a sphere centered in the base platform center (see blue dotted lines in Fig. 3). The two servomotors have the motor shaft connected to the distal revolute joint on two legs, providing the above mentioned 2-DoF actuation. The legs equipped with the servomotors have an active rotation on the lower joint and a passive rotation on the other three joints. By varying the actuation of the servomotors, the moving platform can reach any position within its workspace.

An additional servomotor is located on the moving platform, actuating a spiral-cam mechanism that in turn actuates the chosen end-effector through three joint plates on three joint sliders. The spiral cam is rigidly mounted to the servomotor shaft to effectively push the joint bases along their guide-rails. When the cam is turned, the joint bases slide radially, changing the overall diameter of the joint space, indicated as a red circle in Fig. 3. The guide channels allow the joint bases to reach a minimum diameter of 56 mm to a maximum of 106 mm. These dimensions are set by the mechanical constraints on the three legs; increasing the diameter would consequently reduce the height of the coupling parallel mechanism which, in turn, reduces the diameter of the spherical curve of the moving platform workspace (Fig. 3b).

Table. I shows the main technical specifications of the device. A video of the device in action is available as supplemental material and at https://youtu.be/7reybpCVQdg.

TABLE I
TECHNICAL SPECIFICATIONS

Length × Width × Height	12 × 12 × 15 cm
Control system	M5Stack Core2, ESP32
Operating voltage range	6.0 V
Operating joints speed	0.14 sec/60°
Workspace	Spherical curve, radius 13-15 cm

B. The shape-changing end-effectors

As mentioned before, this device has been designed to support a wide range of end-effectors. As a representative example, we present two interchangeable end-effectors: a soft end-effector (E1 in Fig. 1), rendering different curvatures, and a rigid origami-like end-effector (E2 in Fig. 1), rendering different folding shapes. The end-effectors are installed on the joint sliders through passive revolute joints as shown in Fig. 2a and Fig. 2.

1) Soft Y-shaped end-effector: This end-effector is composed of a flexible equilateral Y-shaped strip of PolyFlex TPU90, with a thickness of 1.5 mm. It is shown in Figs. 1 (E1) and 4. The end-effector strip is attached onto the joint plates through three stoppers (see Fig. 2). Because of the radial movement of the joint bases, the Y-shaped strip is forced to bend towards the vertical direction (positive z_p axis) when the spiral cam rotates. A mechanical stopper prevents the Y-shaped strip to deform in the downward direction. By adjusting the material characteristics of the Y-shaped strip (i.e, dimension, thickness), we can easily render different ranges of curvatures and stiffness.

2) Origami-inspired rigid end-effector: The design of this end-effector is inspired by a modular origami structure. Such surface can fold/unfold to render specific reconfigurable structures. It is shown in Figs. 1 (E2), 5, and 6. To control the rendered shape, a kinematic-based description of the origami

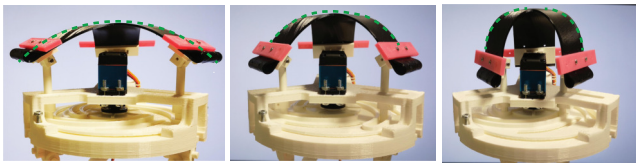

Fig. 4. Soft Y-shaped end-effector. It is composed of a 3D printed Y-shaped strip attached to the moving platform through three joint sliders actuated by the servomotor through a spiral cam. When the spiral cam rotates, the diameter of the circle encompassed by the joint sliders changes, controlling the curvature of the end-effector (in green).

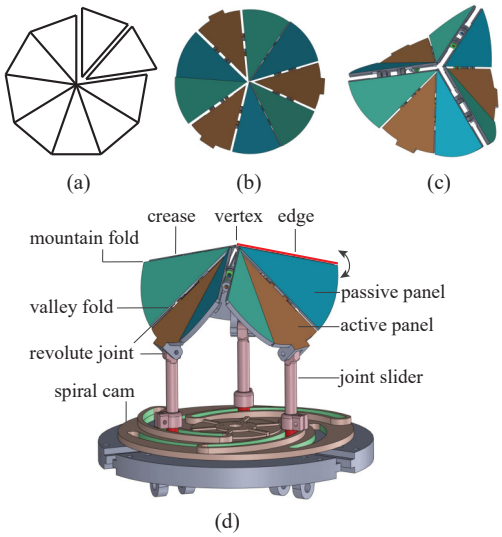

Fig. 5. Origami-inspired rigid end-effector: the design. In (a) the single triangular panels are jointed together to form a modular re-configurable surface. Such a surface can render different edges as the spiral cam rotates. In (b, c, d) the folding of the end-effector is controlled by rotating the spiral cam, which in turn moves the joint sliders towards the center of the platform. Doing so, the end-effector goes from flat to folded, rendering three edges and a center vertex. Of course, by changing the origami structure, we can render different reconfigurable shape sensations.

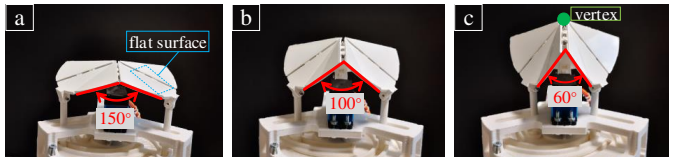

Fig. 6. Origami-inspired rigid end-effector: folding action. The folding of the end-effector is controlled by rotating the spiral cam, which in turn moves the joint sliders towards the center of the platform. Doing so, the end-effector goes from flat (150° angle between two adjacent passive panels, left figure) to folded (60° angle between two adjacent passive panels, right figure), rendering three edges and one vertex.

can be obtained [27]. We designed a structure composed of nine identical flat circle sectors (referred to as "panels" in Fig. 5), connected to each other with revolute joints, so as to bend into edges and one vertex in the center. Three of these panels are connected to the three actuated joint sliders through revolute joints. The sector angle per each actuated panel covers 40°, and it is linked to two passive panels as shown in Fig. 5.

When the joint sliders move, the active panels contract in unison approaching to the center of the spiral cam O_p (see Fig. 3). Doing so, the connection between the passive triangular elements folds them into a mountain-fold (creating an edge, see Fig. 5). Of course, different origami structure can lead to a wide range of reconfigurable surfaces.

C. Hardware

The device is realised using standard rapid prototyping techniques. All passive mechanical components on the device are 3D printed, using Polylactic Ascid lastic (PLA) and

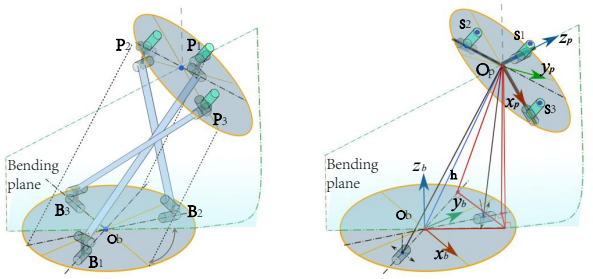

(a) Simplified schematic of the 3-4R mechanism.

(b) Kinematic model on the two actuating legs.

Fig. 7. Kinematic scheme of the proposed device (no end-effector).

Thermoplastic Polyurethane (TPU) filament with Stratasys (F370) and PRUSA 3D printer.

The device is actuated by 6V position-controlled servomotors (ZOSKAY 35 kg·cm torque), two are rigidly mounted to the base platform while the motor shafts are connected to the revolute joints of two legs. The third servomotor is mounted on the moving platform, with the shaft aligned to Z_p and centered in O_p, and drives the spiral cam directly to ensure a high torque transmission. An M5Stack (M5Stack Technology Co., Ltd) integrated controller governs the actuation of all the servomotors, and directly manages the position control.

IV. Characterisation of the End-Effectors

For the characterisation of the end-effectors, let us consider the center of the moving platform O_p, as shown in Figs. 3 and 7a. Observing the Fig. 7b, we called O_b the center of the base platform, which is connected in B_1, B_2, B_3 to the moving platform, through the three legs. The device enables points P_i to have variable reciprocal distance dependant on the diameter $d(\gamma)$ of the slider circle (the circle encompassed by the joint sliders), where γ is the rotation angle of the spiral cam located at the center of the moving platform.

Since the joint sliders are constrained in the symmetrical guides of the spiral cam (see Fig. 2d), the positions of the sliders depend on the spiral-cam mechanism rotational angle γ, driven by the servomotor placed on the moving platform. As an example, when γ is zero, the distance of the joint sliders from the center is $d_m/2 = 28$ mm. The spiral cam mechanism can rotate until reaching a maximum rotation of $2\pi/3$ by moving the joint sliders away from O_p, to a maximum distance of $d_M/2 = 53$ mm from O_p. This movement actuates the end-effector attached to the joint sliders according to its specific kinematics and characteristics.

Below we analyze how this motion affects the two representative end-effectors that we consider in this paper. On the other hand, the direct and inverse kinematics of the three-legged parallel mechanism can be easily derived using reciprocal screw system theory, similarly to [24].

A. Soft Y-shaped end-effector

As the spiral cam rotates and the joint sliders get closer to each other and to the center of the platform, the end-effector bends, rendering spherical shapes of increasing curvatures. Let

us consider a rendered curve $\mathcal{C}(x_{E_1}, R)$ having a curvature $1/R$ at the top of the bent end-effector.

The second order equation $\hat{f}(x_{E_1}) = ax_{E_1}^2 + bx_{E_1} + c$ (where b can be null) that best fits the rendered shape (for a limited sector) can be obtained as:

$$\min_{a,c} ||\mathcal{C}(x_{E_1}, R) - \hat{f}(x_{E_1})||^2. \quad (1)$$

The integral relation

$$\int_0^{\frac{x_{E_1}}{2}} \sqrt{1 + (d\hat{f}(x_{E_1})/dx_{E_1})^2} dx_{E_1} = d_M/2, \quad (2)$$

describes a generic parabolic curve with length $d_M/2$, where $d_M = 106$ mm is the maximum diameter for the slider circle. From there, we can directly obtain x_{E_1} using the Newton-Raphson method and, from the following:

$$x_{E_1} = \frac{d(\gamma)}{2}, \quad (3)$$

we obtain γ value for the servomotor.

B. Origami-inspired end-effector

Similarly as before, also the configuration of this end-effector depends on the distance of joint sliders from the O_p center and, consequently, by γ, i.e., the rotation angle of the servomotor on the moving platform. In particular, for the considered origami structure, shown in Figs. 5 and 6, the configuration is constrained at the three anchoring points located on the joint sliders. As the distance between the joint sliders and the center O_p decreases, the angle of the mountain-fold (edge) decreases towards a value of 60°, with $d(\gamma) = d_m$ when $\gamma = 0°$. The minimum value of the angle (so the "sharpest" configuration of the structure, as shown in Fig. 6c) is obtained when the vertex is raised 20 mm along the positive direction of z_p (as in Fig. 6c).

Note that as the spiral cam rotates and the joint sliders gets closer to each other, points P_i get closer to each other, lowering the moving platform. This behavior can be seen in the accompanying video.

V. User Study on the Soft Y-Shaped End-Effector

We carried out a user study to evaluate the rendering capabilities of the soft Y-shaped end-effector, evaluating its capabilities in generating distinguishable spherical shapes with variable curvatures.

Twelve subjects (10 males, 2 females, aged 22-31) were enrolled in the experiment. Ten of them had little experience with haptic devices (used once a year), two of them had extensive experience with haptic devices (used once a month). Participants used their dominant hand to interact with the device (seven right hand, five left hand).

TABLE II
User Study. Radii (mm) of the spherical surfaces rendered using the soft Y-shaped end-effector.

(40,45) (40,50) (40,55) (40,60)	(75,80) (75,85) (75,90) (75,95)
(45,40) (45,50) (45,55) (45,60)	(80,75) (80,85) (80,90) (80,95)
(50,40) (50,45) (50,55) (50,60)	(85,75) (85,80) (85,90) (85,95)
(55,40) (55,45) (55,50) (55,60)	(90,75) (90,80) (90,85) (90,95)
(60,40) (60,45) (60,50) (60,55)	(95,75) (95,80) (95,85) (95,90)

A. Experimental setup

The static platform of the device is fixed on a table, as shown in Fig. 8. Participants sit in front of the table, able to comfortably reach the end-effector of the device. Participants were also asked to wear an eye mask to prevent the participant from seeing the movement of the end-effector. The experimenter controlled the device and recorded the answer given by the participants.

B. Methods and protocol

We aim at exploring the difference in curvature participants can perceive when interacting with the soft Y-shaped end-effector. We considered a set of curvatures spanning the whole rendering workspace of the device. The spiral cam can move the joint sliders to encompass circles (see Fig. 3) with diameters from 56 mm to 106 mm, generating curvatures having radii from 30 to 100 mm on the soft end-effector surface (see Sec. IV-A). Using a standard two-alternative forced choice (2AFC) design, we proposed the participants to interact with two curvatures, one after the other, having differences in radii of 5, 10, 15, and 20 mm. Participants were asked to identify which one had the larger curvature. We considered 40 comparisons, each repeated two times, listed in Table II. For each comparison, participants were asked to touch the first surface with their palm for 5 seconds (see Fig. 9), then break contact with the surface, and then touch the second surface for another 5 seconds. Participants were allowed to interact with the surface as they liked during the 5-seconds interactions.

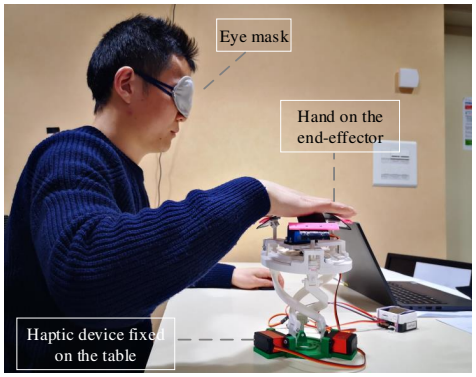

Fig. 8. User study. Experimental setup showing a user interacting with the end-effector. Users were not able to see the device moving.

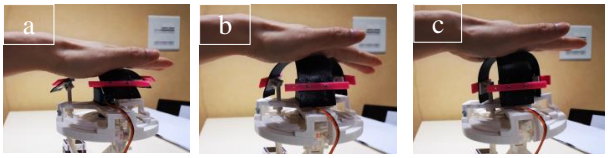

Fig. 9. User study. The soft Y-shaped end-effector render the sensation of interacting with three different curvatures. From (a) to (c), the rendered curvature increases (and its radius decreases).

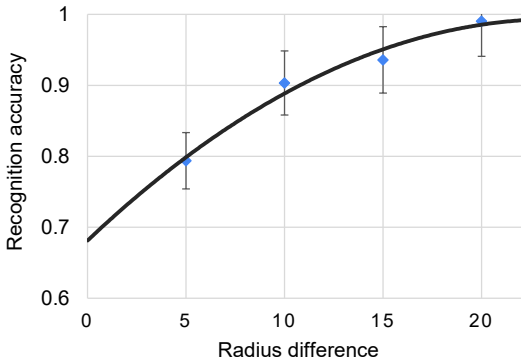

Fig. 10. User study on the soft Y-shaped end-effector. The accuracy of the recognition as a function of the difference in the presented curvatures radii difference (mm). Mean and standard deviations are plotted.

C. Results

Figure 10 shows the recognition accuracy registered during the experiment. As expected, as the difference between the curvatures increases, it is easier to correctly identify which one has the larger curvature. Results reveal that participants gave higher recognition accuracy when the radius difference increases from 5 mm to 20 mm. This result also indicates that the two renderings with more radius difference are easier to distinguish than the one with less difference.

VI. Use case: encounter-type interaction with re-configurable surfaces

To showcase the device capabilities in delivering on-demand haptic touch sensations, we designed a use case study where participants interacted with virtual objects in a three-dimensional environment.

The base platform of the device was fixed on a table as in the previous experiment. Participants were asked to wear a HTC Vive tracker on their wrist, so as to track the position of the hand. The experimental setup is shown in Fig. 11. The device follows the movement of the hand, so as to always face the palm of the user, ready for the interaction.

VII. Discussion and Conclusion

We presented the "Haptic Mushroom", a 3-DoF grounded shape-changing encounter-type haptic device designed for interchangeable end-effectors that can be easily and manually exchanged to provide the sensation of touching curved or slanted surfaces with the palm. The device can supports several end-effectors. As a representative example, we presented two

Fig. 11. Use case: encounter-type interaction with re-configurable surfaces. The motion of the user's hand was tracked by the HTC Vive motion system. The base platform of the device was fixed on a table and the moving platform follows the hand so as to always face the user's palm, ready for interaction.

end-effectors in this paper: a soft end-effector, able to change its curvature, and a rigid origami-inspired end-effector, able to change its shape from flat to sharp.

With respect to existing solutions, the proposed device combines the characteristics of encounter-type devices with those of shape-changing/reconfigurable interfaces. Moreover, the possibility of easily adapting the end-effector to the target haptic sensations makes the device quite flexible and applicable to a broad range of scenarios.

A user study enrolling 12 participants evaluated the performance of the soft end-effector in rendering different curvatures, showing over 90% recognition accuracy when rendering curvatures that differed 0.1 mm^{-1} or more. A use case scenario showed the potential of using the device in rendering virtual shapes during a free-hand encounter-type interaction. Users shown a sufficient capability in distinguishing curvature ranges and angular surfaces with the presented device, showing its viability in virtual and remote interactions.

One of the limitations of the proposed interface is its workspace, which results to be quite small. However, the size of the spherical surface onto which the upper platform moves can be easily modified by adjusting the length of the legs. Moreover, thanks to the light weight of the device, it can be also attached to a standard robotic arm for interactions in much larger workspaces. Another limitation is in its actuation and 3D printer structure. Using DC motors instead of servomotors and sturdier materials would guarantee higher position control accuracy. Finally, while the current prototype has only been tested in perceptual experiments, it can also be suitable for guidance applications, e.g., rendering the presence of virtual and physical fixtures during remote manipulation or mobile robotic guidance.

Acknowledgments

This work was supported by the European Union's Horizon Europe research and innovation program under grant agreement No. 101070066 (REGO) and the China Scholarship Council No. 201908440309.

REFERENCES

[1] V. R. Mercado, M. Marchal, and A. Lécuyer, "Haptics On-Demand: A survey on encountered-type haptic displays," *IEEE Trans. Haptics*, vol. 14, no. 3, pp. 449–464, 2021, doi:10.1109/TOH.2021.3061150.

[2] M. K. Rasmussen, E. W. Pedersen, M. G. Petersen, and K. Hornbæk, "Shape-changing interfaces: a review of the design space and open research questions," in *Proc. the SIGCHI Conference on Human Factors in Computing Systems*, 2012, doi:10.1145/2207676.2207781, pp. 735–744.

[3] R. Suzuki, E. Ofek, M. Sinclair, D. Leithinger, and M. Gonzalez-Franco, "Hapticbots: Distributed encountered-type haptics for vr with multiple shape-changing mobile robots," in *Proc. ACM Symposium on User Interface Software and Technology (UIST)*, 2021, doi:10.48550/arXiv.2108.10829, pp. 1269–1281.

[4] X. de Tinguy, T. Howard, C. Pacchierotti, M. Marchal, and A. Lécuyer, "Weatavix: wearable actuated tangibles for virtual reality experiences," in *Haptics: Science, Technology, Applications: 12th International Conference, EuroHaptics*, 2020, 10.1007/978-3-030-58147-3_29, pp. 262–270.

[5] E. Bouzbib, M. Teyssier, T. Howard, C. Pacchierotti, and A. Lécuyer, "Palmex: Adding palmar force-feedback for 3d manipulation with haptic exoskeleton gloves," *IEEE Transactions on Visualization and Computer Graphics*, 2023, 10.1109/TVCG.2023.3244076.

[6] V. Hayward and O. R. Astley, "Performance measures for haptic interfaces," in *Robotics research: The seventh international symposium*, 1996, doi:10.1007/9781447142256, pp. 195–206.

[7] C. Pacchierotti, S. Sinclair, M. Solazzi, A. Frisoli, V. Hayward, and D. Prattichizzo, "Wearable haptic systems for the fingertip and the hand: taxonomy, review, and perspectives," *IEEE Trans. haptics*, vol. 10, no. 4, pp. 580–600, 2017,doi:10.1109/TOH.2017.2689006.

[8] M. Marchal and C. Pacchierotti, "Virtual reality and haptics," in *Robotics Goes MOOC*, B. Siciliano, Ed., 2022.

[9] J. Yin, R. Hinchet, H. Shea, and C. Majidi, "Wearable soft technologies for haptic sensing and feedback," *Advanced Functional Materials*, vol. 31, no. 39, p. 2007428, 2021, doi:10.1002/adfm.202007428.

[10] M. Malvezzi, F. Chinello, D. Prattichizzo, and C. Pacchierotti, "Design of personalized wearable haptic interfaces to account for fingertip size and shape," *IEEE Trans. Haptics*, vol. 14, no. 2, pp. 266–272, 2021, 10.1109/TOH.2021.3076106.

[11] C. Pacchierotti, E. M. Young, and K. J. Kuchenbecker, "Task-driven pca-based design optimization of wearable cutaneous devices," *IEEE Robotics and Automation Letters*, vol. 3, no. 3, pp. 2214–2221, 2018, 10.1109/LRA.2018.2810953.

[12] V. Mercado, M. Marchal, and A. Lécuyer, "Entropia: towards infinite surface haptic displays in virtual reality using encountered-type rotating props," *IEEE Trans. visualization and computer graphics*, vol. 27, no. 3, pp. 2237–2243, 2019, doi:10.1109/TVCG.2019.2963190.

[13] R. Meguro, P. Ratsamee, T. Mashita, Y. Uranishi, and H. Takemura, "Frictionhaptics: Encountered-type haptic device fortangential friction emulation," in *2019 IEEE International Symposium on Mixed and Augmented Reality Adjunct (ISMAR-Adjunct)*, 2019, doi:10.1109/ISMAR-Adjunct.2019.000-6, pp. 382–383.

[14] B. Araujo, R. Jota, V. Perumal, J. X. Yao, K. Singh, and D. Wigdor, "Snake charmer: Physically enabling virtual objects," in *Proc. the TEI'16: Tenth International Conference on Tangible, Embedded, and Embodied Interaction*, 2016, doi:10.1145/2839462.2839484, pp. 218–226.

[15] L. Zhang, Y. Liu, H. Bai, Q. Zou, Z. Chang, W. He, S. Wang, and M. Billinghurst, "Robot-enabled tangible virtual assembly with coordinated midair object placement," *Robotics and Computer-Integrated Manufacturing*, vol. 79, p. 102434, 2023, doi:10.1016/j.rcim.2022.102434.

[16] E. J. Gonzalez, P. Abtahi, and S. Follmer, "Reach+ extending the reachability of encountered-type haptics devices through dynamic redirection in vr," in *Proc. the 33rd Annual ACM Symposium on User Interface Software and Technology (UIST)*, 2020, doi:10.1145/3379337.3415870, pp. 236–248.

[17] L. H. Kim and S. Follmer, "Swarmhaptics: Haptic display with swarm robots," in *Proc. CHI Conference on Human Factors in Computing Systems*, 2019, doi:10.1145/3290605.3300918, pp. 1–13.

[18] H. Iwata, H. Yano, F. Nakaizumi, and R. Kawamura, "Project feelex: adding haptic surface to graphics," in *Proc. the 28th annual conference on Computer graphics and interactive techniques*, 2001, doi:10.1145/383259.383314, pp. 469–476.

[19] I. Poupyrev, T. Nashida, S. Maruyama, J. Rekimoto, and Y. Yamaji, "Lumen: interactive visual and shape display for calm computing," in *ACM SIGGRAPH 2004 emerging technologies*, 2004, doi:10.1145/1186155.1186173, p. 17.

[20] K. Nakagaki, D. Fitzgerald, Z. Ma, L. Vink, D. Levine, and H. Ishii, "inforce: Bi-directional force/shape display for haptic interaction," in *Proc. International Conference on tangible, embedded, and embodied interaction*, 2019, doi:10.1145/3294109.3295621, pp. 615–623.

[21] S. Follmer, D. Leithinger, A. Olwal, A. Hogge, and H. Ishii, "inform: dynamic physical affordances and constraints through shape and object actuation." in *Proc. ACM Symposium on User Interface Software and Technology (UIST)*, vol. 13, no. 10, 2013, doi:10.1145/2501988.2502032, pp. 2501–988.

[22] M. Blackshaw, A. DeVincenzi, D. Lakatos, D. Leithinger, and H. Ishii, "Recompose: direct and gestural interaction with an actuated surface," in *Proc. Extended Abstracts on Human Factors in Computing Systems*, 2011, pp. 1237–1242.

[23] M. Okada and Y. Nakamura, "Development of a cybernetic shoulder-a 3-dof mechanism that imitates biological shoulder motion," *IEEE Trans. Robotics*, vol. 21, no. 3, pp. 438–444, 2005, doi:10.1109/TRO.2004.838006.

[24] L. Kuang, M. Marchal, M. Aggravi, P. R. Giordano, and C. Pacchierotti, "Design of a 2-dof haptic device for motion guidance," in *Haptics: Science, Technology, Applications: 13th International Conference on Human Haptic Sensing and Touch Enabled Computer Applications, EuroHaptics 2022, Hamburg, Germany, May 22–25, 2022, Proceedings*. Springer, 2022, pp. 198–206.

[25] L. Kuang, M. Marchal, P. R. Giordano, and C. Pacchierotti, "Rolling handle for hand motion guidance and teleoperation," in *EuroHaptics 2022-International Conference on Haptics: Science, Technology, Applications*, 2022.

[26] Y.-J. Kim, J.-I. Kim, and W. Jang, "Quaternion joint: Dexterous 3-dof joint representing quaternion motion for high-speed safe interaction," in *2018 IEEE/RSJ International Conference on Intelligent Robots and Systems (IROS)*. IEEE, 2018, doi:10.1109/IROS.2018.8594301, pp. 935–942.

[27] R. L. P. Barreto, F. V. Morlin, M. B. de Souza, A. P. Carboni, and D. Martins, "Multiloop origami inspired spherical mechanisms," *Mechanism and Machine Theory*, vol. 155, p. 104063, 2021, doi:10.1016/j.mechmachtheory.2020.104063.